Reuse of a wing venation gene-regulatory network in patterning the eyespot rings of butterflies

Tirtha Das Banerjee [1, *], Seah Kwi-Shan[1], and Antónia Monteiro[1,2, *]

Affiliations

1 Department of Biological Sciences, National University of Singapore, Singapore - 117557.

2 Science Division, Yale-NUS College, Singapore - 138527.

* Authors for correspondence

Email: tirtha_banerjee@u.nus.edu, antonia.monterio@nus.edu.sg

Abstract

Novel organismal traits might reuse ancestral gene-regulatory networks (GRNs) in their development, but data supporting this mechanism are still sparse. Here we propose that a conserved venation gene network, used in patterning insect wings, has been recruited to pattern the sharp and distinct rings of color in butterfly eyespot development. This network involves Decapentaplegic (Dpp), acting as a central morphogen, activating *optix* and *spalt* at different concentration thresholds. It also involves Spalt cross-regulating *optix* resulting in the formation of a sharp boundary between the two genes. First, using *in situ* hybridizations, we show that *dpp* is expressed in the eyespot centers during the early pupal stage and that CRISPR-Cas9 embryonic knockouts of *dpp*, *optix*, and *spalt* result in the loss of eyespots, loss of the orange ring, and loss of the black scales, respectively. Furthermore, using RNAi during the pupal stage, we show that *dpp* down-regulation results in the complete or partial loss of eyespots. Using CRISPR disruptions of *optix* or *spalt*, followed by immunostainings, we show that Spalt represses *optix* in the central region of the eyespot, limiting *optix* expression to a more peripheral ring. We further illustrate that *optix* disruptions alter scale pigmentation and scale ultrastructure as they transform orange to brown scales. Altogether, the regulatory interactions between *dpp*, *spalt* and *optix* mimic those found in earlier larval developmental stages, in the anterior compartment of an insect's wing, where these genes play a role in venation patterning. The network similarities suggest that the venation GRN was co-opted to aid in the differentiation of the eyespot rings.

Keywords

optix, *decapentaplegic*, *spalt*, co-option, positional information, eyespots, *Bicyclus anynana*

Introduction

While it is possible that novel organismal traits emerge from the gradual construction of dedicated gene-regulatory networks (GRNs), one gene being added at a time, such networks may instead emerge from pre-existing clusters of pre-wired genes that are repurposed during development. So far, a few examples of this mechanism of GRN co-option have been proposed for the development of novel complex traits. These include the reuse of a GRN that differentiates breathing spiracles in *Drosophila* larvae in the development of the posterior lobe of adult genitalia (Glassford et al., 2015); the reuse of the leg GRN in patterning the wings of insects (Bruce and Patel, 2020; Clark-Hachtel and Tomoyasu, 2020) or the head horns of beetles (Zattara et al., 2016); the reuse of the wing GRN in the development of a treehopper's

helmet (Fisher et al., 2020); or the reuse of an appendage GRN to pattern butterfly eyespot centers (Murugesan et al., 2021).

Eyespots, unlike the other examples of appendage co-option, where the novel trait protrudes from the body, do not grow out of the wing (**Figure 1A**). This means that either only a small core network of genes shared between appendages and eyespots was co-opted in the first place, or that the similarities in the development of these traits break apart later in development, after the eyespot centers have differentiated in the late larval stage. One mechanism for this to happen is if another network gets rewired downstream of the shared core network to produce a novel output, i.e., to differentiate rings of color around the central signalling cells rather than tissue outgrowth. Here we explore whether the network of genes involved in early vein patterning in butterflies could have been repurposed to differentiate the color rings in eyespots at later stages of development.

The mechanism of vein patterning in *Bicyclus anynana* butterflies has many similarities to that of *Drosophila*, which is a classic example of positional-information in developmental biology (Blair, 2007). In both flies and butterflies, the morphogen Decapentaplegic (Dpp) is expressed in a stripe in the middle of the larval wing, along the anterior-posterior compartment (Zecca et al., 1996; Banerjee and Monteiro, 2020a). In flies, Dpp activates multiple genes in the anterior compartment of the third instar wing disc, including the transcription factors *spalt* and *optix* at different concentration thresholds (Martín et al., 2017). The cross-regulatory interaction between these two genes determines the sharp boundaries that eventually position one of the longitudinal veins, L2 (Martín et al., 2017). In butterflies, the expression of Spalt and Optix proteins is also found surrounding a stripe of *dpp* expression, in homologous patterns to those in flies (Banerjee and Monteiro, 2020a), suggesting a conserved vein patterning mechanism in both insects.

The same three genes, *dpp, spalt* and *optix*, might also be involved in a positional information mechanism, similar to the one described above, but used in the differentiation of butterfly eyespot rings.. In this mechanism, a morphogen secreted from the center of the eyespot activates a series of genes at different concentration thresholds and distance from the center (Nijhout, 1978; Brunetti et al. 2001). One of the hypothesised morphogens was inferred to be a member of the BMP (Bone Morphogenetic Protein) signaling pathway (which includes Dpp) because a BMP pathway transducer protein, phosphorylated Mothers against decapentaplegic (pMad), was visualized at high levels in the eyespot central cells (Monteiro et al., 2006). A potential target of this BMP morphogen could be *spalt (sal)*, a gene that is expressed in a broad disc around the central cells and required for black disc differentiation (Brunetti et a. 2001; Murugesan et al, 2021). No study, however, has shown the expression or function of any BMP ligand in eyespot centers nor of *optix* in eyespot ring differentiation, despite this latter gene being associated with the development of red and orange color patterns in other butterflies (Reed et al., 2011; Zhang et al., 2017).

In this study we tested the hypothesis that the vein patterning GRN, involving Dpp as a central signaling molecule, and *spalt* and *optix* as target genes, might have been co-opted in the differentiation of eyespots rings. We first used *in situ* hybridizations to investigate the expression of *dpp* in *Bicyclus anynana* butterflies, in the early pupal stages. We then used CRISPR-Cas9 applied in the early embryo and early pupal wing, as well as RNAi applied in the early pupal wing, to test the function of *dpp* in eyespot development and ring differentiation. We then targeted the other known candidate downstream target of Dpp signaling (in vein differentiation), *optix*, with CRISPR, to test its function in eyespot development. Finally, we targeted both *spalt* and *optix*, in turn, and followed these disruptions with visualizations of the presence of both proteins in the eyespot field, to test for a potential functional interaction in

color ring differentiation similar to that observed in differentiation of the L2 vein in *Drosophila* (Martín et al., 2017).

Results

Expression and function of *decapentaplegic* (*dpp*) in the eyespot center

To explore whether *dpp* might be expressed in eyespot centers we performed *in-situ* hybridization at different stages of pupal development. We found *dpp* expression in the eyespot centers in a 18-24 hrs time window after pupation (**Figure 1B**). This time window overlaps the window of development when Spalt proteins are observed in the black scale cells (Monteiro et al., 2006; Brunetti et al., 2001). This coincident temporal expression is interesting as *spalt* is a target of Dpp in vein development (Blair 2007).

To test the function of *dpp* in eyespot development we used CRISPR-Cas9. Knocking out *dpp* by injecting a single guide RNA (sgRNA) and Cas9 during the embryonic stages proved to be extremely difficult and resulted in high embryonic mortality. This is likely due to *dpp* being involved in patterning the early embryos (Ashe et al., 2000). We overcame this high lethality by first injecting a sgRNA-Cas9 mixture in late embryos (4-6 hrs after egg laying) and second, by injecting the sgRNA-Cas9 mixture into 3-6 hr old pupae, just prior to eyespot ring differentiation.

Late embryonic knockouts of *dpp* resulted in one individual with the loss of an anterior hindwing eyespot, increases in the size of two other eyespots (one being the large Cu1 eyespot), loss of either M1 or M2 veins, incomplete development of M1/M2 and M3 veins (**Figure S1**), and the appearance of ectopic silver scales (**Figure 1D and E, Figure S1**). These phenotypes are partially similar to *Ultrabithorax (Ubx)* knockout phenotypes (Matsuoka and Monteiro, 2021), that essentially transform a hindwing into the morphology of a forewing, leading to the ectopic appearance of silver scales, and changes in eyespot number and size.

To overcome a potential role of *dpp* in early wing identity specification, through a potential interaction with *Ubx*, and to further elucidate the role of *dpp* as an eyespot central morphogen during the pupal stage, we performed CRISPR-Cas9 experiments during the pupal stage (see methods for details). *dpp* knockouts during this stage resulted in one individual showing the loss of the Cu2 hindwing eyespot (**Figure 1F**) and another without the M1 forewing eyespot (**Figure 1H**), along with defects in wing veins, consistent with vein differentiation functions in *Drosophila* and *Bicyclus* (**Figure S1**) (Banerjee and Monteiro, 2020a). This suggests that *dpp* is required for eyespot development during the pupal stage, when *dpp* is expressed in the eyespot centers.

To strengthen these CRISPR-Cas9 results we performed RNAi using two siRNAs designed to knock-down the levels of *dpp*. Delivery of the siRNAs into cells was mediated by a Lipofectamine RNAiMAX reagent. These pupal injections led to the loss of eyespots, and to a smaller eyespot with no black ring (**Figure 1K-M**). One of the lost eyespots (Cu1) was the same eyespot that had increased in size with embryonic injections. Using qPCR, we confirmed the reduction in the levels of *dpp* transcripts in the wing tissue, despite these being non-significant ($n = 4$; $F=0.5676$; $p =0.239$) (**Figure 1N**). This result might be due to the expression of *dpp* being restricted to a few cells of the eyespot centers, at this stage of wing development **(Figure 1B)**, which is challenging to quantify with a whole-wing qPCR assay.

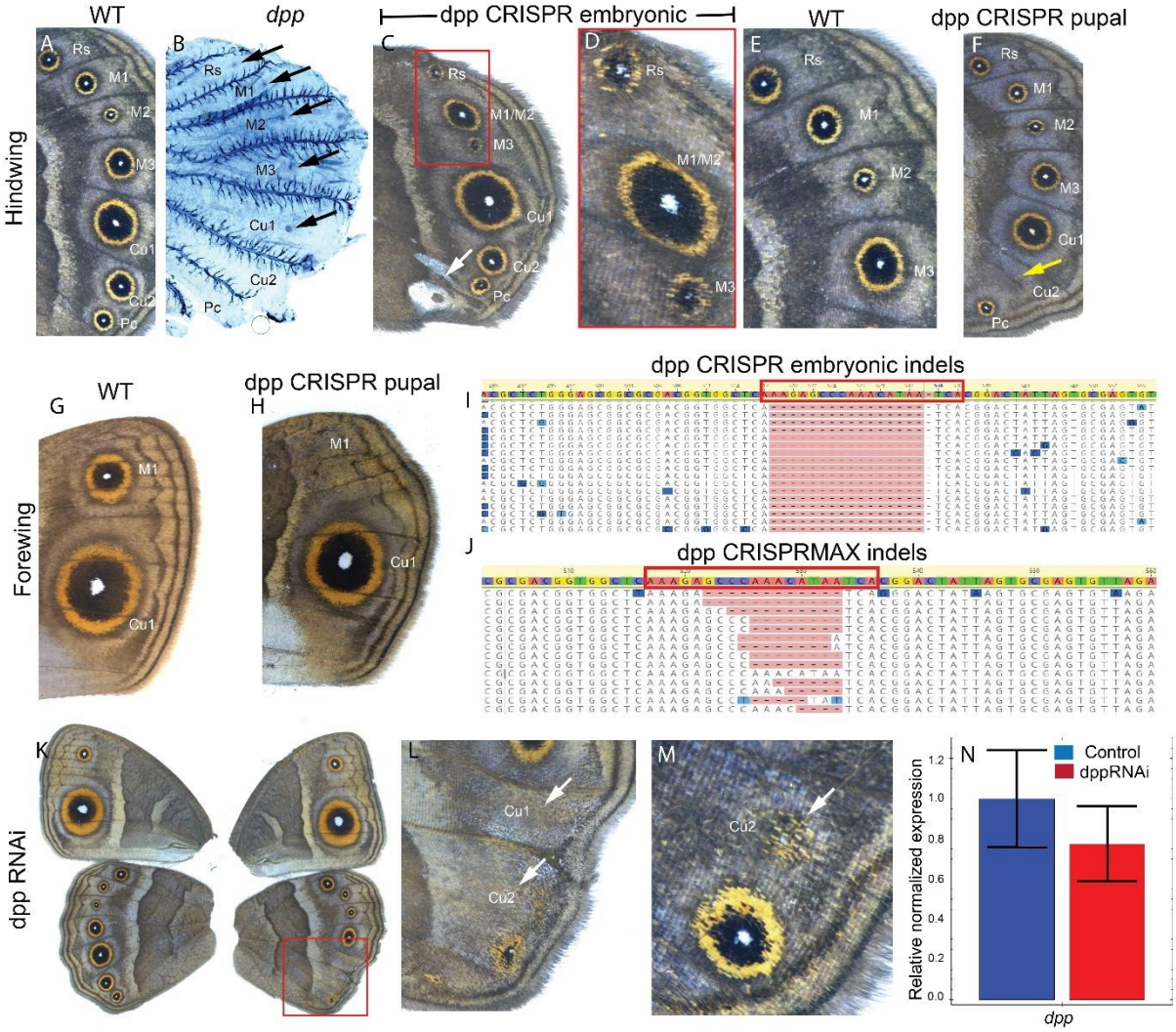

Figure 1. Expression and function of *decapentaplegic (dpp)*. (A) Adult WT. **(B)** Expression of *dpp* in the eyespot centers of an 18 hrs old pupal hindwing. **(C and D)** CRISPR-Cas9 knockout of *dpp* during embryonic development resulted in the loss of either the M1 or M2 eyespot, increases in size of two eyespots M1 (or M2) and Cu1, and` ectopic appearance of silver scales (white arrow). (**E**) Adult WT hindwing. (F) Loss of Cu2 eyespot (yellow arrow) due to CRISPR knockout in the pupal stage. (**G)** WT adult forewing. **(H**) Loss of the M1 eyespot in the forewing (blue arrow) due to CRISPR knockout in the pupal stage. (**I**) Deletions (red shaded region) at 3 bps 5' of the PAM site of *dpp* guide RNA site (boxed area) obtained using DNA extracted from the wing shown in panels C and D. (**J**) Deletions (red shaded region) at 3 bps 5' of the PAM site of *dpp* guide RNA using CRISPRMAX reagent. Tissue was obtained from the wing in panel **F**. (**K, L**) RNAi using siRNA designed against *dpp* results in the loss of two eyespots in the injected region (white arrows). (**M**) Reduction in eyespot size with loss of black scales (white arrow) in the *dpp* RNAi injected site. (**N**) qPCR on wing tissue treated with *dpp* RNAi shows reduction in the levels of *dpp* compared to control injected wings.

Expression and function of Optix and Spalt proteins in the forewing and hindwing eyespots

To examine the temporal and spatial expression of Optix and Spalt proteins in eyespots we used immunostainings. Optix protein was observed prominently in the orange ring of both the forewing and hindwing eyespots from 24-72 hrs **(Figure 2C-F, K-M**) of pupal development. The presence of Optix in the center of the eyespot was only observed in a few individuals during the 24-hr time window. Very faint Optix levels were observed in the eyespot center nuclei after 24 hrs pupal development (**Figure 2L and M**). Spalt was present in the black scale cells of the forewing and hindwing at least till 24 hrs of the pupal wing development (**Figure 2G-J, N-P**), as previously reported (Brunetti et al. 2001; Monteiro et al. 2006).

To test the function of *optix* and *spalt* we used injections of CRISPR-Cas9 into early embryos. Individuals that emerged from these injections were mosaics where some cells were disrupted for *optix* and *spalt* function whereas others were wildtype. For *optix,* some individuals showed transformation of their orange-colored scales to a brown color (**Figure 2Q-T**). For *spalt,* some individuals developed orange scales in the black scale region of the eyespots (**Figure 2W-Z**), as previously shown (Murugesan et al. 2021). To confirm that the loss of orange color corresponded to a loss of Optix protein in cells of the orange ring, we performed immunostains against Optix in some of the injected animals at the pupal stage of development. This revealed that Optix protein was missing from cells of the orange ring of the eyespots (**Figure 2U and V**). Finally, we confirmed that knocking out *optix* and *spalt* led to deletion of nucleotides mostly near the targeted sites (**Figure 2AA, AB, and AC**). These results show that both *optix* and *spalt* are required for the development of the orange and black rings of scale cells, respectively. They also suggest that Spalt might be repressing the expression of *optix* in the central black disc domain, because in *spalt* crispants, these central black scale cells become orange.

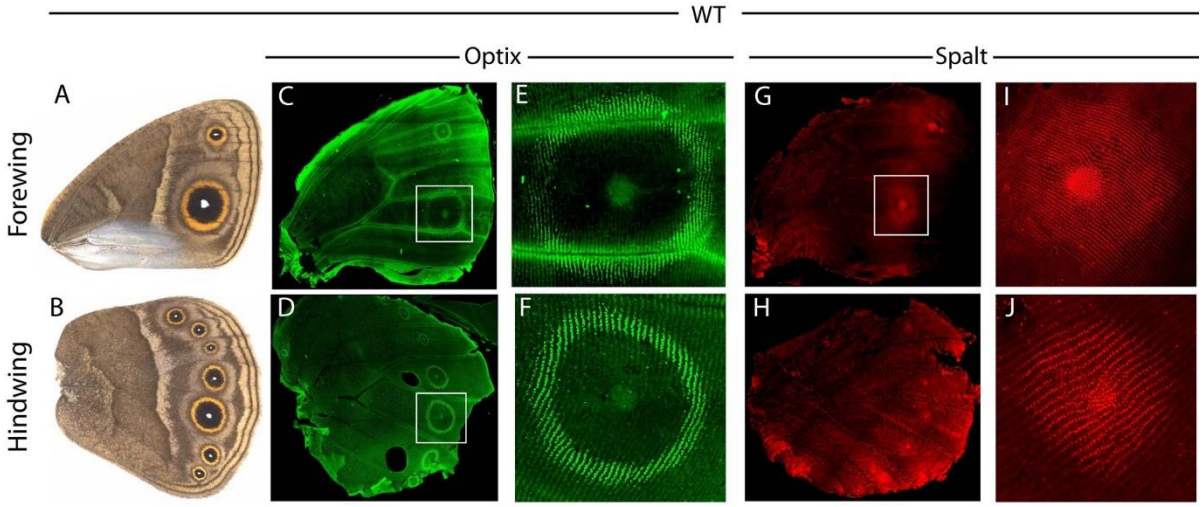
WT
Optix
Spalt
A
C
E
G
I
Forewing
B
D
F
H
J
Hindwing

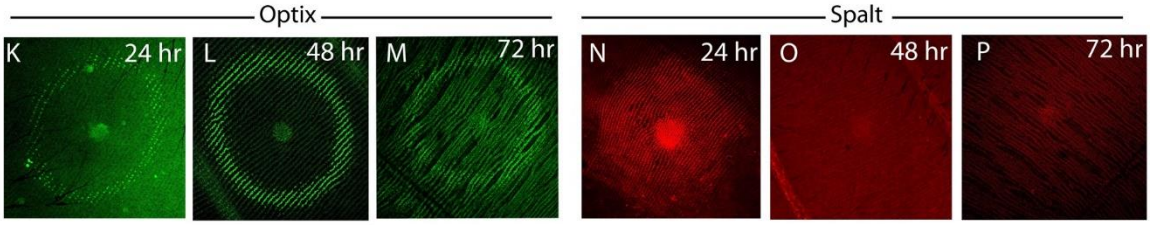
Optix
Spalt
K 24 hr
L 48 hr
M 72 hr
N 24 hr
O 48 hr
P 72 hr

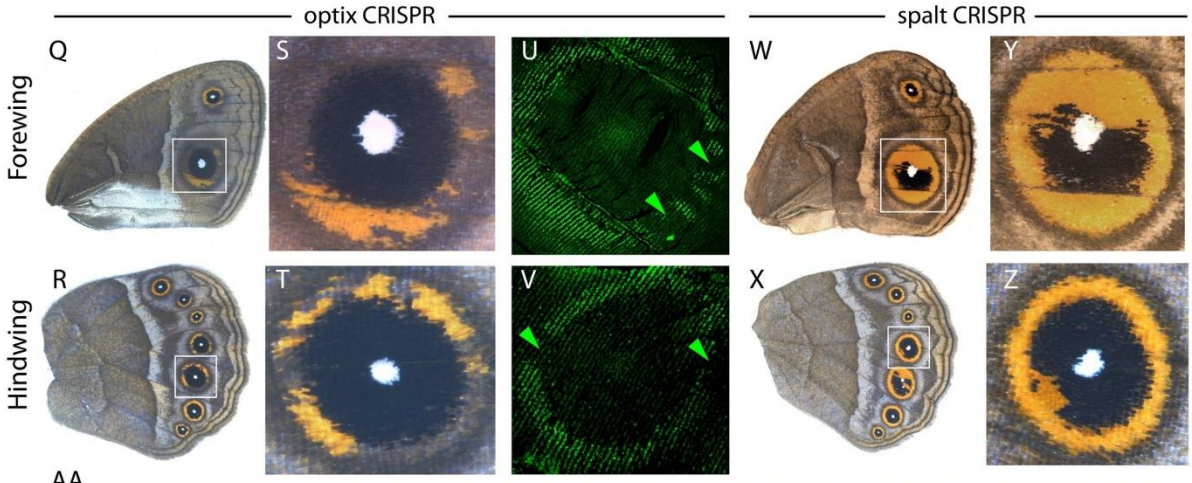
optix CRISPR
spalt CRISPR
Q
S
U
W
Y
Forewing
R
T
V
X
Z
Hindwing

AA
optix CRISPR indels
Optix WT Bicyclus
AB
Optix WT Bicyclus

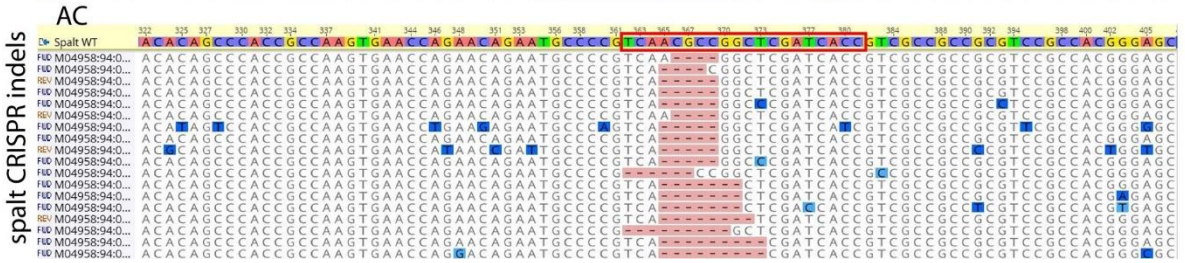
AC
spalt CRISPR indels
Spalt WT

Figure 2. Expression and function of Optix and Spalt proteins in the forewing and hindwing eyespots. (A) WT forewing, **(B)** WT hindwing. **(C)** The presence of Optix proteins in the forewing and **(D)** in the hindwing. **(E and F)** Presence of Optix in the orange ring of Cu1 eyespots (boxed in C and D). (**G**) Presence of Spalt protein in the forewing and **(H)** in the hindwing. **(I and J)** Presence of Spalt protein in the black disc of Cu1 eyespots (boxed in G and H). (**K-M**) Optix proteins are present till 72 hrs of pupal development in the orange ring of the eyespots. (**N-P**) Spalt proteins are present in the black scale cells till 24 hrs of pupal development, after which levels go down. (**Q-T**) CRISPR-Cas9 knockout of *optix* produced defects in the development of the eyespot's orange ring in both wings (S, T are amplified photos of the eyespots boxed in Q, R). (**U and V**) *optix* CRISPR results in the loss of Optix protein in cells of the future orange ring area of the eyespots. (**W-Z**) CRISPR-Cas9 knockout of *optix* in the forewing and hindwing produces defects in the development of the eyespot's black scales. Orange scales develop inside the black scale domain. CRISPR deletions at the **(AA and AB)** *optix* and (**AC**) *spalt* target sites in three distinct individuals.

The interaction of *optix* and *spalt* in the eyespots

To further investigate whether *spalt* is repressing *optix* from its own expression domain, we first examined the co-expression of Optix and Spalt proteins more closely, with double immunostainings. In *B. anynana,* Spalt protein is present in a central disc of cells in the eyespots (**Figure 3G**), immediately surrounded by a ring of Optix protein (**Figure 3D**) in flanking cells (**Figure 3J**). In some individuals, faint levels of Optix are also observed in the center of the eyespots at 16-24 hrs pupal wing development (**Figure 3D and F**).

To test the regulatory interaction between *spalt* and *optix* in eyespots, we performed knockouts of each gene in turn, followed by immunostainings targeting the protein products of both genes. *optix* crispants showed loss of orange pigments in the orange scales **(Figure 3B),** loss of Optix proteins in cells of the orange ring **(Figure 3E),** but did not show changes in the area of black scales (**Figure 3B**), or in the presence of Spalt proteins in those cells (**Figure 3H and K**). These data indicate that *optix* is involved in giving the orange ring its color, but this gene is likely not involved in regulating the outer perimeter of the eyespot's black disc nor *spalt* expression in the eyespots. *spalt* crispants showed the development of orange scales in the black scale region of the eyespots **(Figure 3C),** loss of Spalt protein **(Figure 3I)**, and ectopic levels of Optix protein in the black scale disc region **(Figure 3F and L; Figure S2E)**. These data indicate that *spalt* represses *optix* expression in the central black disc region of the eyespot, where loss of *spalt* leads to activation of *optix* in this region and to a change in scale color from black to orange.

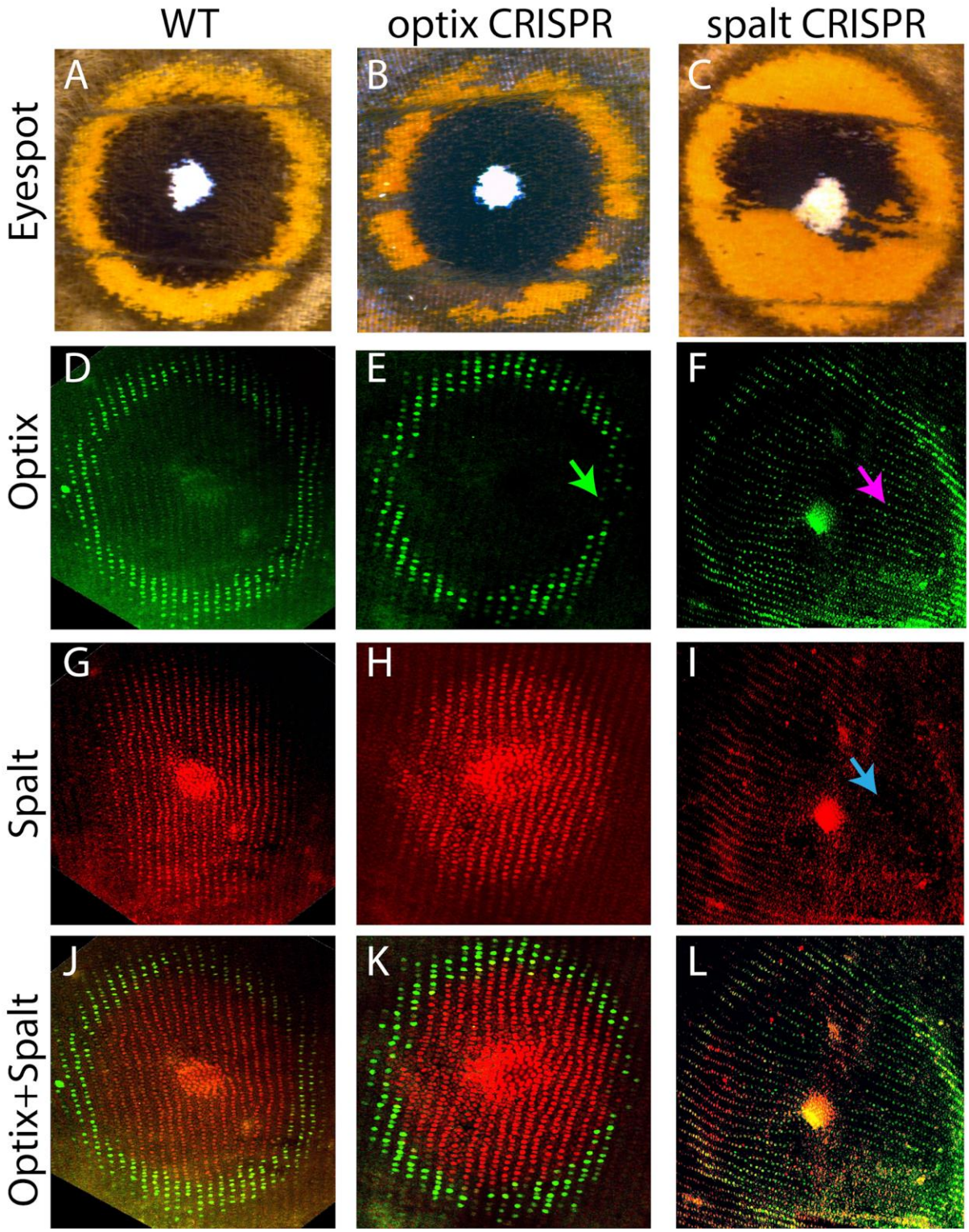

Figure 3. Spalt protein prevents *optix* from being expressed in the black disc region of the eyespot (16-20 hrs pupal development). **(A)** WT eyespot, **(B)** *optix* crispant, and **(C)** *spalt* crispant. **(D-F)** Eyespots stained with an antibody against Optix in WT *optix* crispant and *spalt* crispant individuals. **(G-I)** Eyespots stained with an antibody against Spalt in WT, *optix* crispant and *spalt* crispant individuals. **(J-L)** Merged channels of Spalt and Optix. Green arrow marks the region of missing Optix protein in the *optix* crispant individual. The presence of

Spalt protein is not affected due to the absence of Optix in adjacent cells. Pink arrow marks the ectopic presence of Optix, where Spalt proteins are missing (blue arrow).

Both Optix and Spalt proteins are present in the center of the eyespots in some individuals where the respective genes show a different interaction (**Figure 2J and L**). Disruptions of *optix*, however, don't produce any defects in the pigmentation and scale ultrastructure of these central white scales (**Figure S2, and Figure S5**), indicating that the presence of Optix in these scales has no clear function. Disruption of *sal*, however, results in the development of orange scales in the white center of the eyespots (**Figure S3F-I**).

Transformation of scale structure and changes in pigmentation in the eyespots due to *optix* knock-out

To further explore the role of *optix* in the transformation of the orange scales into brown scales we examined the differently colored scales in eyespots using a scanning electron microscope (SEM) and a spectrophotometer. Knocking-out *optix* resulted in the loss of a thin upper lamina that connects the crossribs in part of the upper surface of the orange scales (**Figure 4B and C**). This modification made these scales resemble the morphology of WT brown scales (**Figure 4D**). The structure of black and white scales, however, was not affected (**Figure S2**). Knocking out *optix* also resulted in a change of the absorbance spectra of the wing from orange to brown at the orange scale region resembling the color of WT brown scales (**Figure 4E**). This indicates that brown, likely melanin pigments, replaced the orange pigments, in these scales. The gene *optix*, thus, regulates both the pigments and the morphology of the orange scales.

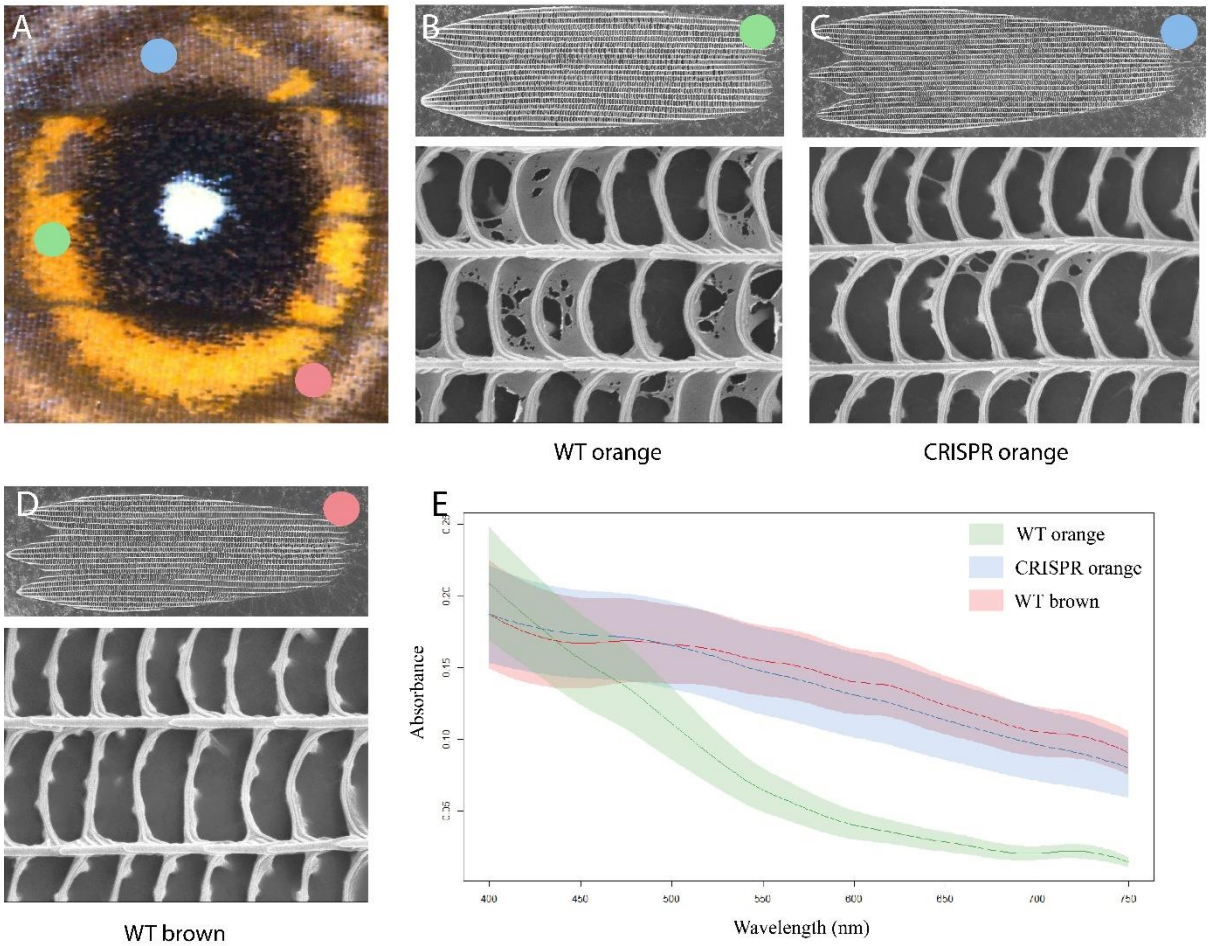

Figure 4. *optix* promotes the development of a thin upper lamina and of orange pigments in the orange scales. (**A**) *optix* knockout results in the conversion of orange scales into brown scales. SEM images of (**B**) an orange scale from the orange ring, (**C**) an *optix* CRISPR modified scale from the same ring, and (**D**) a brown scale from an outer ring. Knocking out *optix* results in the reduction of a thin upper lamina found in orange scales, and thicker crossribs, making these scales resemble the morphology of brown scales. (**E**) Absorbance spectra of WT and optix CRISPR scale patches. Knocking-out *optix* results in the conversion of the absorbance spectra of orange scales to that of brown scales, indicating a change in pigments. The color shading around the black curves indicates the standard deviation of the spectral measurement for each scale type from four individuals. Colored dots represent the areas used for scale sampling and spectrophotometric analysis.

Discussion

A wing venation gene network was likely co-opted to pattern eyespot rings

Our study proposes that the genetic circuit involving *dpp*, *spalt* and *optix*, complete with its cross-regulatory interactions, may have been co-opted from a vein patterning function, in the early larval wings of butterflies, to eyespot ring differentiation in the later pupal stage.

Eyespot ring differentiation has been hypothesized to involve a centrally produced morphogen since 1978 (Nijhout, 1978), but the identity of that morphogen has remained elusive. Here we developed a technique to knockout *dpp* only during the early pupal wing to show that *dpp* is essential for ring differentiation in the early pupal stage. We used the Lipofectamine CRISPRMAX reagent (see methods for detail) to transfer both a sgRNA-Cas9 mix and siRNA to the pupal wing cells. The knockout and knockdowns resulted in the complete or partial loss of eyespots (**Figure 1F, H, K, L, and M**), indicating that Dpp is required for eyespot ring development, including the development of the central white scales.

We then found other parallels between the expression and function of the genes that are expressed around the central Dpp region in eyespots, *spalt* and *optix*, and those expressed around a similar, albeit linear, region in early vein patterning in *Drosophila* and *Bicyclus* (Martín et al., 2017, Banerjee and Monteiro, 2020b; **Figure 5A, B**). In both systems, *dpp* is expressed in a stripe of cells along the A-P boundary in early wings, and the proteins Spalt and Optix are expressed in bands at progressive distances from this central stripe. Functional perturbations of *dpp*, *spalt* and *optix* in *Drosophila* and *Bicyclus*, showed they all played a role in wing growth and vein patterning (Banerjee and Monteiro, 2020a; Barrio and De Celis, 2004; Ingham and Fietz, 1995; Martín et al., 2017).

Here we showed that the mechanism of ring differentiation in an eyespot also requires these three genes, and that the regulatory interactions between at least two of these genes are conserved in vein and eyespot ring patterning. In particular, we showed the central expression of *dpp* in eyespots, and the requirement for that gene in the development of all the color rings in an eyespot. Furthermore, we showed that the regulatory interaction between *spalt* and *optix* observed in early larval wing discs of *Drosophila*, where *spalt* represses *optix* and keeps it out of its expression domain (Martín et al., 2017), is present in the eyespots of *Bicyclus* **(Figure 5A**). In particular, Spalt is repressing the activation of *optix* in the black scale area. In the *Drosophila* wing disc, a similar down-regulation of *spalt* with RNAi led to the expansion of the Optix domain in the anterior compartment (Martín et al., 2017). In *Bicyclus*, disruptions of *optix* led to the loss of Optix protein in the orange ring precursor cells, but did not affect the

expression domain of Spalt (**Figure 3**). These results are also consistent with *Drosophila* wing vein patterning, where downregulation of *optix* with RNAi did not affect the spatial domain of Spalt (Martín et al., 2017). Overexpression of *optix*, however, reduced the Spalt domain in the wing disc (Martín et al., 2017), suggesting that Optix can also repress *spalt*, if expressed at high levels in the same cells.

The phenotypes we observed with embryonic *dpp* knockouts suggest that *dpp* is perhaps also involved in establishing hindwing identity. Knockouts of *dpp* during the embryonic stages proved quite challenging due to *dpp's* role in embryonic development (Ashe et al., 2000). The single crispant individual we obtained had fewer hindwing eyespots but also had other eyespots enlarged, making that hindwing resemble a forewing. The loss of the M1 (or M2) eyespot was likely due to the complete loss of Dpp along one vein (either the M1or M2 vein) (**Figure S1**) (Banerjee and Monteiro, 2020a). However, the hindwing acquiring forewing features, such as enlarged M1/M2 and Cu1 eyespots, and the development of silver scales in the posterior compartment (**Figure 1C and D, and Figure S1**), are not consistent with a mere eyespot development function for *dpp*. We propose that these features could be due to an interaction between *Ubx* and *dpp*, as a previous *Ubx* crispant in *B. anynana* showed a similar phenotype (Matsuoka and Monteiro, 2021). In *Drosophila*, Ubx, a Hox gene responsible for hindwing identity, controls both the transcription and mobility of Dpp in the haltere (Crickmore and Mann, 2006). We propose that Ubx is playing a similar role in *Bicyclus* hindwings during the larval stage. At this stage, *dpp* expression surrounds the expression of Armadillo (a Wnt transducer) and Distal-less proteins in the eyespot centers (Connahs et al., 2019). The increase in size of M1 and Cu1 eyespots with *dpp* knockouts (**Figure 1C and D**) could be due to the proposed role of Dpp proteins in restricting the expression of these two other genes to the eyespot centers via a reaction-diffusion mechanism (Connahs et al., 2019). If Dpp proteins are removed, the centers might be able to expand, leading to larger eyespots. Also, if Ubx is regulating both *dpp* expression and mobility, *dpp* knockouts will mimic *Ubx* knockouts.

In the pupal stage, however, *dpp* is expressed in the center of the eyespots, not in cells around the center, as in larval stages, and appears to have a different function. Our pupal knockout and knockdown data suggest that *dpp* is involved in differentiating all the rings of the eyespots at this stage, as we observe reduction or deletion of eyespots with *dpp* disruptions (**Figure 1F, H, K, and M**). This gene appears, thus, to have different roles in eyespot development during the larval and pupal stage: it has a focal size differentiation function during the larval stage and a focal signalling function in the pupal stage.

Two roles are also observed for *sal:* in eyespot center differentiation during the larval stage, and in the differentiation of the black disc during the pupal stage. Sal might be playing a role in a proposed reaction-diffusion mechanisms proposed for focus differentiation during the larval stages (Connahs et al. 2019), where knockouts result in loss of eyespots (Murugesan et al. 2022) or in split eyespot centers (**Figure S3J**). During the pupal stage, however, disruptions of *sal* lead to transformation of black to orange scales, via the *sal-optix* cross-regulatory mechanism identified here.

Here we also showed that *optix* regulates both the color and the microstructure of the orange scales. *Optix* has been previously described to play a role in scale pigmentation of *Heliconius erato, Agraulis vanilla, Vanessa cardui* and *Junonia coenia* butterflies where *optix* knockouts resulted in the loss of red and orange pigments and in the downregulation of key ommochrome pigmentation genes and upregulation of melanin genes (Reed et al., 2011; Zhang et al., 2017). In our experiments, the orange pigment, likely an ommochrome, was substituted by a brown pigment, (**Figure 4A and E**), likely a melanin. Optix appears, thus, to have a conserved function to act as a switch to toggle the production of ommochromes and melanins across

butterflies (Zhang et al., 2017). Our results also show that *optix* alters the morphology of orange scale cells in a novel way. In *Bicyclus*, *optix* is required to form a cuticle lamina that partially covers the windows or spaces between the crossribs (the upper lamina) of the orange scales (**Figure 4C**). Previous work in *Junonia coenia* showed that *optix* was involved in determining the thickness of the lower lamina of background orange/brown scales, where disruptions of *optix* resulted in increased thickness of the lower lamina along with pigmentary changes (Thayer et al., 2020). *optix*, thus, appears to function in thinning the lower lamina in *Junonia*, and in building the upper lamina in *Bicyclus* scales. A recent study, however, proposed that *optix* produces both effects simultaneously in silver scales in *Bicyclus*: it thins the lower lamina and thickens the upper lamina (Prakash et al., 2021).

Several knowledge gaps still remain surrounding eyespot ring differentiation. Support for the vein network GRN co-option proposed in this study would benefit from testing whether *optix* and *sal* are responding to Dpp signals produced at the center of the eyespots. It is also unclear whether Dpp and Wingless are jointly required for eyespot ring differentiation. Wingless is another proposed morphogen for eyespot development (Monteiro et al., 2006; Özsu et al., 2017) and its function should be newly investigated using knockouts. In addition, the role Engrailed (En) in eyespot ring differentiation, a gene co-expressed in the same orange cells as Optix, is still unclear (Brunetti et al., 2001) (**Figure S7**). Multiple paralogs are expressed in eyespots (Banerjee and Monteiro 2020), and disruptions of all paralogs simultaneously may need to be performed to overcome functional redundancy.

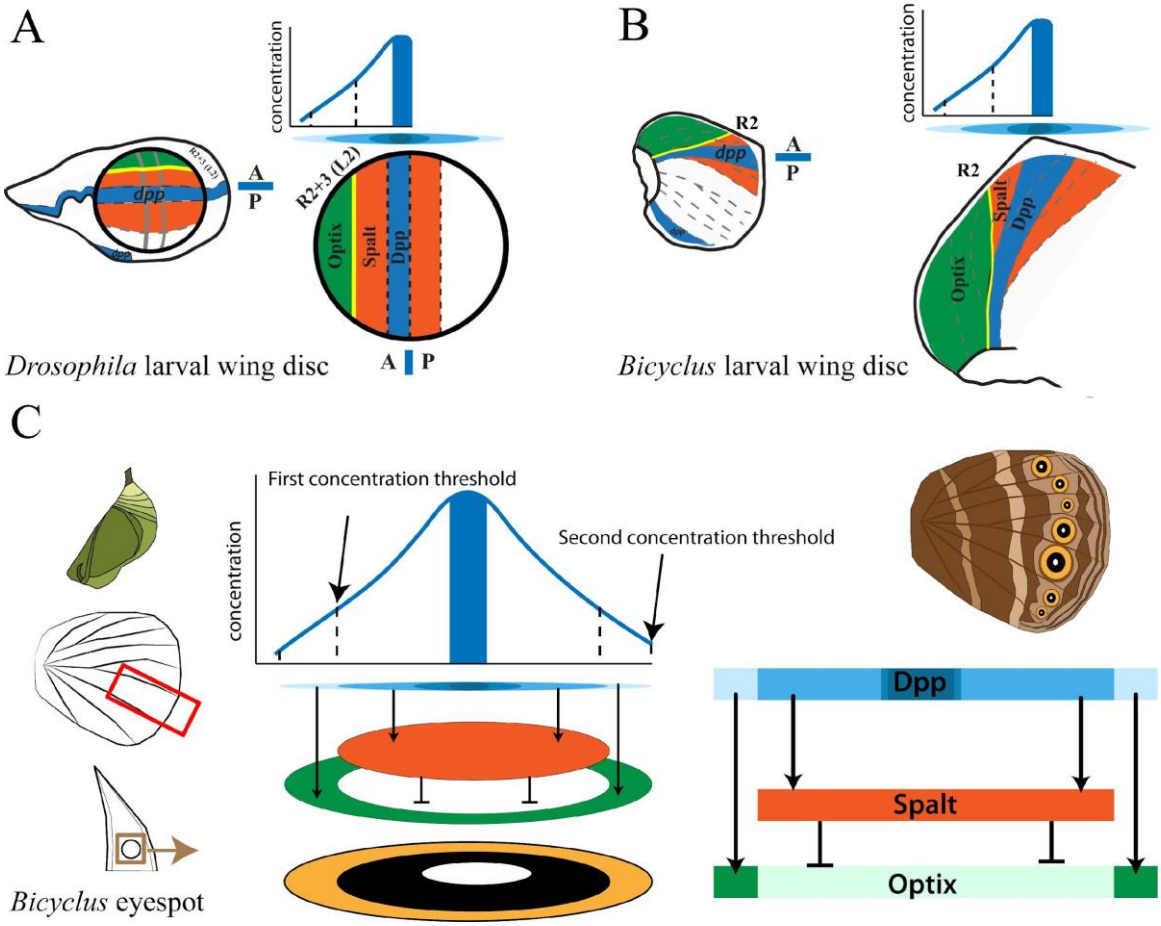

Figure 5. A positional information model for the eyespot pattern formation via a mechanism similar to the anterior-posterior wing network. (A) Positioning of *Drosophila* R2+3 (L2) vein via Dpp (blue). Dpp diffuses from the AP boundary and activates *spalt* (orange)

and *optix* (green) at different concentration threshold. Spalt represses the activation *optix* in cell's posterior to the vein L2. Cells in between Spalt and Optix domains expresses *knirps* (co-repressed by Spalt and Optix) which leads to the development of L2 provein cells (Martín et al., 2017). **(B)** Proposed positioning of *Bicyclus* R2 vein via Dpp (blue) via the same mechanism as discussed above for *Drosophila* (Banerjee and Monteiro, 2020a). **(C)** A mechanism identical to that involved in patterning the AP axis of the wing might be involved in eyespot ring differentiation. In the eyespots the *dpp* gene (blue) is expressed in the central cells. The Dpp protein might act as a morphogen diffusing to the surrounding tissues and activating *spalt* and *optix* at different concentration thresholds. Spalt represses the activation of *optix* in the inner black scale area, and as a result, Optix is expressed only in the outer orange ring region.

Methods

Rearing *Bicyclus anynana*

Bicyclus butterflies were raised in the lab at 27°C, 60% humidity and 12-12 hrs day-night cycle. Larvae were fed young corn leaves and adults were fed mashed bananas.

CRISPR-Cas9

optix and *spalt* CRISPR-Cas9 experiments were carried out based on a protocol previously described (Banerjee and Monteiro, 2018). Guides were designed to target the coding sequence of the genes (see the supplementary file for sequences and the regions targeted). A solution containing Cas9 protein (IDT, Cat No. 1081058) and guide RNA, each at a concentration of 300ng/ul, diluted in Cas9 buffer, and a small amount of food dye was injected into 1509 embryos for *optix* and 863 embryos for *spalt* (**Table S1 and S2.**). A few of these injected individuals were dissected at 24 hrs after pupation to perform immunostainings, while the rest were allowed to grow till adulthood. After eclosing, the adults were frozen at -20° C and imaged under a Leica DMS1000 microscope.

Dpp CRISPR-Cas9 experiment were carried out at embryonic and pupal developmental stages. The embryonic experiment was conducted in the same way as mentioned above except a synthetic guide from Integrated DNA Technologies (IDT) was used. Briefly a 20 bp region was selected using the IDT custom guide tool (see supplementary file for sequence). For the preparation of the synthetic guide-Cas9 mixture, the *dpp* guide (crRNA) was mixed with equimolar amount of tracrRNA (IDT), heated at 95°C for 5 mins and cooled to room temperature. Afterward Cas9 enzyme was added and left for 20 mins at room temperature. Non-toxic food dye was added to the mix and injected into the embryos. For knocking out *dpp* during the pupal stage we used a CRISPRMAX reagent (thermo-scientific; Cat No: CMAX00008) along with the *dpp* synthetic guide mentioned above. The *dpp* guide (crRNA) was mixed with equimolar amount of tracrRNA (IDT), heated at 95°C for 5 mins and cooled to room temperature. After that Cas9 enzyme was added and left for 20 mins at room temperature. To the Cas9-guide mix, 10 µl of Cas9 plus reagent (Thermo-scientific; Cat No: CMAX00008) was added, mixed well, and another 10 µl of CRISPRMAX reagent (Thermo-scientific; Cat No: CMAX00008) was added, mixed via pipetting, and immediately injected in between the forewing and hindwing of 3-6 hrs old pupal wings (see **Figure S1I** for the location of injection). The pupae were left at 27°C with 60% humidity and allowed to eclose. After eclosion, the adults were frozen and imaged under a Leica DMS1000 microscope.

For identification of the indels, DNA from the mosaic CRISPants wings were isolated using Omega Tissue DNA extraction kit (Cat No: D3396-01). Afterwards PCR was performed to amplify the region of interest. PCR products were purified and sent to the next generation sequencing facility at Genewiz. After sequencing, the reads were aligned using Geneious 10.0 to the reference WT gene sequences.

RNA interference

For *dpp* RNAi, custom siRNA were designed using the siDirect RNAi tool. Two of the best siRNAs (see **Table S1** for sequence) were ordered from Shanghai GenePharma Co., Ltd. The siRNAs were diluted to 20 nM in molecular grade water. 5 ul of each siRNA were mixed in a 200 µl tube. 10 ul of Lipofectamine RNAiMAX (Cat No: 13778100) was added and mixed via pipetting. Afterwards, 0.5 µl of food grade dye was added and 5 µl of the mix was injected into a proximal region of 3-6 hrs old pupal wings (See **Figure S1I** for the injection site). For control injections, 2.5 µl of molecular grade water mixed with 2.5 µl of Lipofectamine was injected in the other side of the same individual. Individuals were then either dissected after 4 hrs of injection, to observe changes in the levels of *dpp* expression using qPCR, or left till eclosion to observe the adult phenotype.

qPCR analysis

For the qPCR experiment, RNA was isolated from five of the *dpp* RNAi injected wing and five of the control wings using QIAGEN RNA isolation kit (RNeasy Plus Micro Kit; Cat No.: 74034). cDNA was synthesized using the SuperScript™ II Reverse Transcriptase (Cat. No. 18064-014). KAPA SYBR® FAST (Cat No: KK4601) was used for the quantification of *dpp* transcripts. RpS18 was used as standard (see **Table S1** for primer sequence). The Cq values were analysed on Bio-Rad's CFX manager.

Immunostainings

Pupation time was recorded using an Olympus tough tg-6 camera, and pupal wings were dissected at different timepoints after pupation under a Zeiss Stemi 305 microscope in 1x PBS at room temperature based on a protocol previously described (Banerjee and Monteiro, 2020b). Wings were fixed using 4% formaldehyde in fix buffer (see **Table S3** for details), followed by four washes in 1x PBS, five mins each. After the washes, the wings were incubated in block buffer (see **Table S3** for details) at 4ºC overnight. The next day primary antibodies against Optix (1:3000, rat, a gift from Robert D. Reed) and Spalt (1:20000, guinea pig GP66.1), were added in wash buffer and incubated at 4ºC for 24 hrs. The next day anti-rat AF488 (Invitrogen, #A-11006) and anti-guinea pig AF555 (Invitrogen, # A-21435) secondary antibodies at the concentration of 1:500 in wash buffer were added followed by four washes in wash buffer, 20 mins each. Wings were then mounted on an inhouse mounting media (see **Table S3** for details) and imaged under an Olympus fv3000 confocal microscope.

***In-situ* hybridization**

For the visualization of *dpp* expression in pupal wings of *Bicyclus*, pupation time was recorded, and the wings were dissected from 18-24 hrs old pupae in 1x PBS under a Zeiss stemi 305 microscope based on a previously described protocol (Banerjee and Monteiro, 2020b) and transferred to 1xPBST with 4% formaldehyde. After fixation for 30 min the wings were washed three times in 1x PBST for 5 mins each. The wings were then treated with proteinase K and glycine and washed again three times using 1x PBST. After, the wings were gradually transferred into pre-hybridization buffer (see **Table S4** for composition) and heated at 65ºC for

1 hr. Hybridization buffer with a *dpp* probe (see **Table S4** for composition) was added to the wings and they were incubated for 16 hrs at 65ºC. Wings were then washed five times for 30 mins each in pre-hybridization buffer. After washing, wings were moved to room temperature and gradually transferred to 1x PBST and washed in 1x PBST. Afterwards, the wings were incubated in block buffer (see **Table S4** for composition) for 1 hr, followed by addition of anti-digoxygenin (Sigma-Aldrich, Cat No. 11093274910) diluted 1/3000 times in block buffer. After 1 hr of incubation the wings were washed five time, five mins each in block buffer. Finally, wings were transferred to alkaline-phosphatase buffer (see supp table S4 for composition) supplemented with NBT-BCIP (Promega, Cat No. S3771) and incubated in the dark till the development of color. The wings were imaged under a Leica DMS1000 microscope.

Scanning Electron microscopy

A fine metal needle was used to pick scales from adult WT and optix crispant wings. The scales were then mounted on a carbon tape fixed to an SEM stub, platinum coated using JEOL JFC-1600 Auto Fine Coater and imaged under a JEOL JSM-6701F Field-Emission SEM.

Scale absorbance measurements

Individual scales were placed on a glass slide and immersed in clove oil with a refractive index of 1.53. The scales were then covered with a coverslip and absorbance was measured using a Technospex uSight-2000 Microspectroscopy system. Ten scales were measured for each color type, with measurements taken from three areas on each scale. Measurements were analysed using the R package ‘pavo’ (see supplementary file for code).

Authors contribution

TDB and AM designed the experiments, analysed the results, and wrote the manuscript. TDB performed the experiments. SKS measured the absorbance of scales. All the authors read and agreed to the final version of the manuscript.

Funding

TDB and SKS were supported by a Yale-NUS scholarship. This work was supported by the National Research Foundation, Singapore, Investigatorship award NRF-NRFI05-2019-0006 to AM.

Acknowledgements

We would like to thank Robert Reed for the anti-Optix antibody, Lee Ka Yau (SEM facility, Department of Chemistry, NUS) for his help with imaging the SEM samples, and Vinod Saranathan for access to the spectrophotometer. We would like to thank DBS-CBIS confocal facility and Ms. Tong Yan for access and help with the Olympus fv3000 confocal microscope. The authors declare no conflict of interest.

References

Ashe, H.L., Mannervik, M., and Levine, M. (2000). Dpp signaling thresholds in the dorsal ectoderm of the Drosophila embryo. Development *127*, 3305–3312.

Banerjee, T. Das, and Monteiro, A. (2020a). Molecular mechanisms underlying simplification of venation patterns in holometabolous insects. Development dev.196394.

Banerjee, T. Das, and Monteiro, A. (2020b). Dissection of Larval and Pupal Wings of Bicyclus anynana Butterflies. Methods Protoc. *3*, 5.

Banerjee, T., and Monteiro, A. (2018). CRISPR-Cas9 Mediated Genome Editing in Bicyclus anynana Butterflies.

Barrio, R., and De Celis, J.F. (2004). Regulation of spalt expression in the Drosophila wing blade in response to the Decapentaplegic signaling pathway. Proc. Natl. Acad. Sci. U. S. A. *101*, 6021–6026.

Bier, E. (2000). Drawing lines in the Drosophila wing: Initiation of wing vein development. Curr. Opin. Genet. Dev. *10*, 393–398.

Blair, S.S. (2007). Wing vein patterning in Drosophila and the analysis of intercellular signaling. Annu. Rev. Cell Dev. Biol. *23*, 293–319.

Brakefield, P.M., Gates, J., Keys, D., Kesbeke, F., Wijngaarden, P.J., Monteiro, a, French, V., and Carroll, S.B. (1996). Development, plasticity and evolution of butterfly eyespot patterns. Nature *384*, 236–242.

Bruce, H.S., and Patel, N.H. (2020). Knockout of crustacean leg patterning genes suggests that insect wings and body walls evolved from ancient leg segments. Nat. Ecol. Evol. *4*, 1703–1712.

Brunetti, C.R., Selegue, J.E., Monteiro, A., French, V., Brakefield, P.M., and Carroll, S.B. (2001). The generation and diversification of butterfly eyespot color patterns. Curr. Biol. *11*, 1578–1585.

De Celis, J.F. (2003). Pattern formation in the Drosophila wing: The development of the veins. BioEssays *25*, 443–451.

Clark-Hachtel, C.M., and Tomoyasu, Y. (2020). Two sets of candidate crustacean wing homologues and their implication for the origin of insect wings. Nat. Ecol. Evol. *4*, 1694–1702.

Crickmore, M.A., and Mann, R.S. (2006). Hox control of organ size by regulation of morphogen production and mobility. Science (80-.). *313*, 63–68.

Fisher, C.R., Wegrzyn, J.L., and Jockusch, E.L. (2020). Co-option of wing-patterning genes underlies the evolution of the treehopper helmet. Nat. Ecol. Evol. *4*, 250–260.

Glassford, W.J., Johnson, W.C., Dall, N.R., Smith, S.J., Liu, Y., Boll, W., Noll, M., and Rebeiz, M. (2015). Co-option of an Ancestral Hox-Regulated Network Underlies a Recently Evolved Morphological Novelty. Dev. Cell *34*, 520–531.

Hu, Y., Linz, D.M., and Moczek, A.P. (2019). Beetle horns evolved from wing serial homologs. Science *366*, 1004–1007.

Ingham, P.W., and Fietz, M.J. (1995). Quantitative effects of hedgehog and decapentaplegic activity on the patterning of the Drosophila wing. Curr. Biol. *5*, 432–440.

Al Khatib, A., Siomava, N., Iannini, A., Posnien, N., and Casares, F. (2017). Specific expression and function of the Six3 optix in Drosophila serially homologous organs. Biol. Open *6*, 1155–1164.

Martín, M., Ostalé, C.M., and De Celis, J.F. (2017). Patterning of the drosophila L2 vein is driven by regulatory interactions between region-specific transcription factors expressed in response to Dpp

signalling. Dev. *144*, 3168–3176.

Matsuoka, Y., and Monteiro, A. (2021). Hox genes are essential for the development of eyespots in Bicyclus anynana butterflies. Genetics *217*.

Monteiro, A., Glaser, G., Stockslager, S., Glansdorp, N., and Ramos, D. (2006). Comparative insights into questions of lepidopteran wing pattern homology. BMC Dev. Biol. *6*, 52.

Nijhout, H.F. (1978). Wing pattern formation in Lepidoptera: A model. J. Exp. Zool. *206*, 119–136.

Özsu, N., Chan, Q.Y., Chen, B., Gupta, M. Das, and Monteiro, A. (2017). Wingless is a positive regulator of eyespot color patterns in Bicyclus anynana butterflies. Dev. Biol. *429*, 177–185.

Suriya Narayanan Murugesan, Connahs, H., Matsuoka, Y., Gupta, M. das, Huq, M., Gowri, V., Monroe, S., Deem, K.D., Werner, T., Tomoyasu, Y., et al. (2021). Butterfly eyespots evolved via co-option of the antennal gene-regulatory network. BioRxiv.

Zattara, E.E., Busey, H.A., Linz, D.M., Tomoyasu, Y., and Moczek, A.P. (2016). Neofunctionalization of embryonic head patterning genes facilitates the positioning of novel traits on the dorsal head of adult beetles. Proc. R. Soc. B Biol. Sci. *283*.

Zecca, M., Basler, K., and Struhl, G. (1996). Direct and long range action of a DPP morphogen gradient. Cell *87*, 833–844.

Supplementary materials

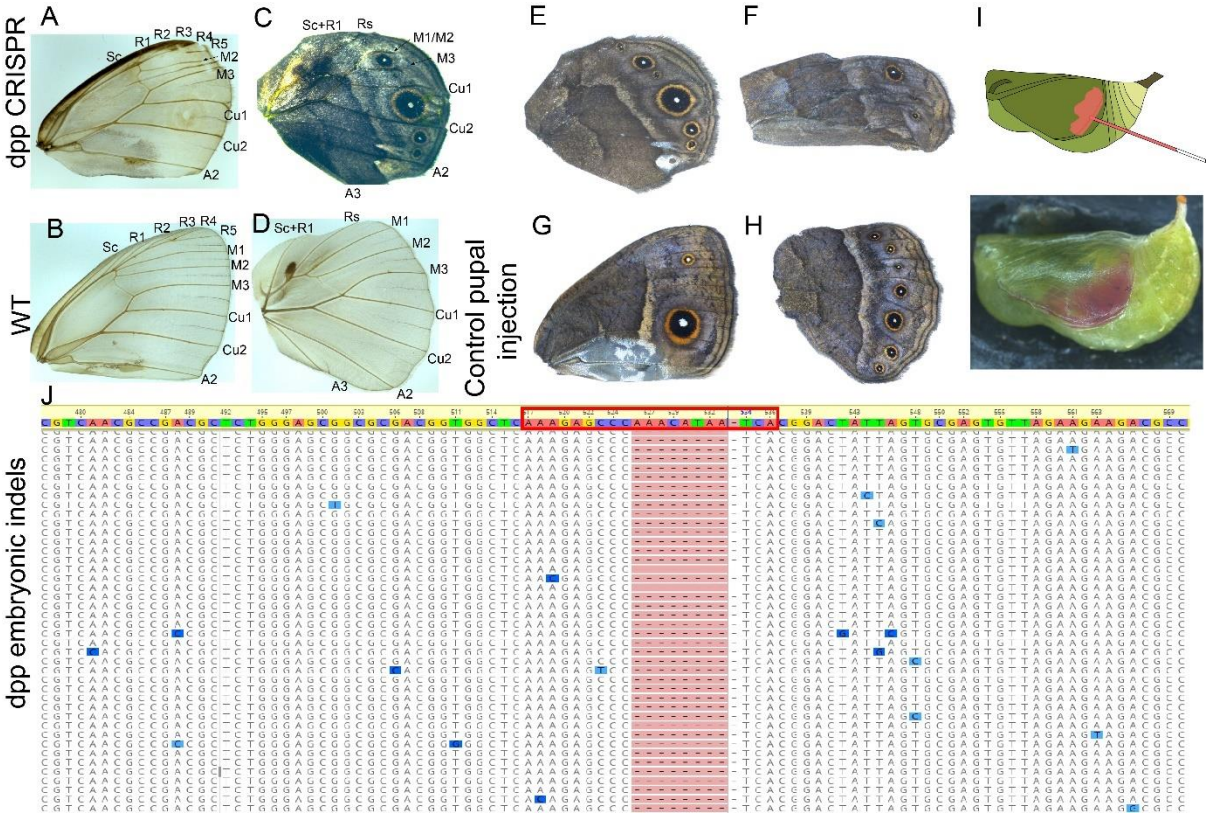

Figure S1: Effect of *dpp* CRISPR on the eyespots. (**A**) Effect of disruptions to *dpp* on adult forewing venation. We observed loss of the M1 vein and incomplete formation of M2 and M3 veins. sgRNA-Cas9 injection was carried out during the pupal stage in this wing. (**B**) WT

adult forewing venation. (**C**) Effect of disruptions to *dpp* on hindwing venation. We observed loss of M1 or M2 veins and incomplete formation of the M1/M2 and M3 veins. (D) WT adult hindwing venation. It is interesting to note that most of the venation defects happen around the anterior-posterior boundary where we observe the strong band of *dpp* expression in larval wings. (**E**) Loss of an eyespot, enlargement of eyespots, and ectopic silver scale development in the hindwing of a *dpp* crispant. (**F**) Extreme wing defect due to disruptions to *dpp*. In C, E, and F sgRNA-Cas9 injections were carried out during the embryonic stage. (**G and H**) Control adult wings with just Cas9 injections along with the CRISPRMAX reagent. The wings develop normally without any defects in the eyespots or in venation. (**I**) Illustration to show the site of injection of sgRNA-Cas9 mix during the 3-6 hrs of pupal wing development. sgRNA-Cas9 mix along with the CRISPRMAX reagent was injected at the center of the wing margin from where the solution slowly diffuses inside the wing. (**J**) Indels at the site of *dpp* CRISPR from the wing in panel **E**.

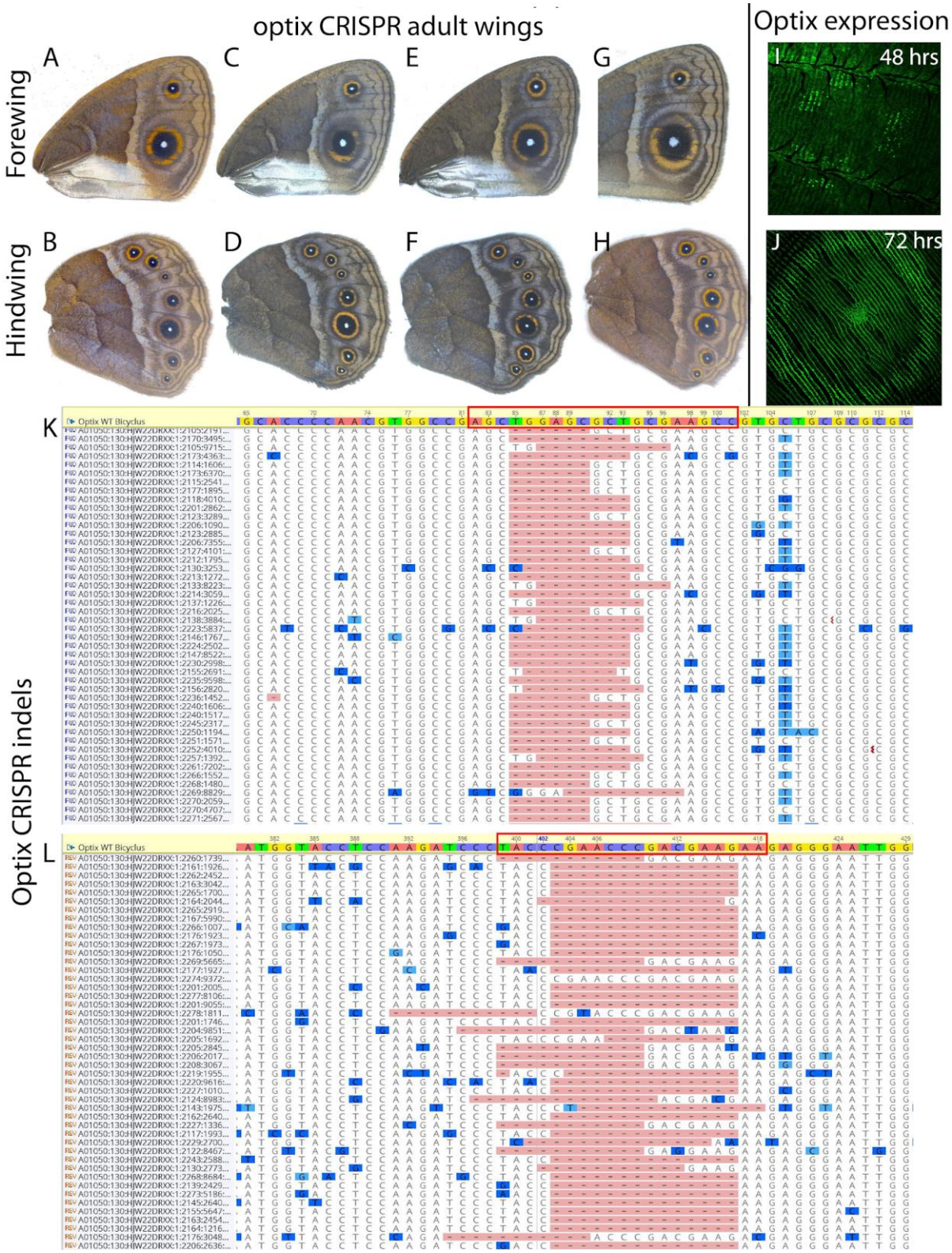

Figure S2. Function of *optix* in *Bicyclus anynana* butterflies and localization of Optix protein in pupal wings. (A-H) *optix* CRISPR adult wings. *optix* CRISPR results in the conversion of orange scales into brown scales in the eyespots. **(I and J)** Antibody staining of Optix proteins in an *optix* CRISPR individual at 48 hrs and a WT 72 hrs old pupal wing. **(K and L)** Deletions at the two sites targeted for *optix* CRISPR.

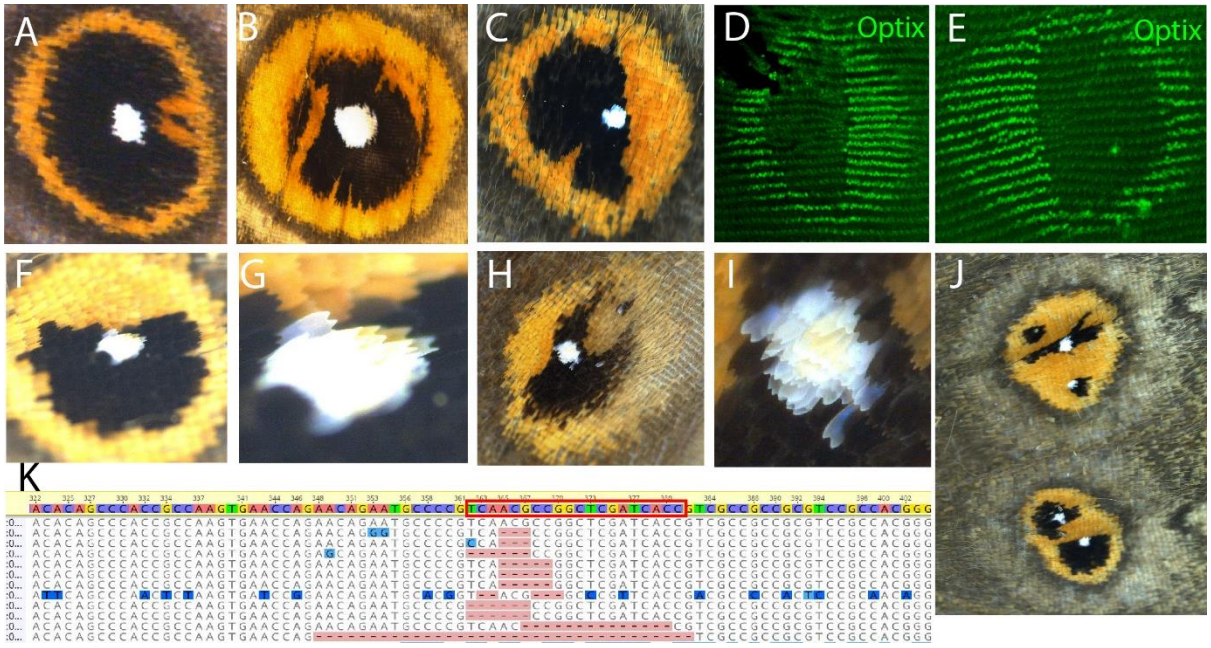

Figure S3: Effect of *spalt* CRISPR on the eyespots. (**A-C**) Loss of Spalt results in the development of orange scales in the black scale region due to the presence of (**D and E**) Optix in that region. (**F-I**) Loss of sal results in the development of yellow scales in the white center scale region of the eyespot. (**J**) Loss of *spalt* results in the split of eyespot foci with distinct domains of the white, black, and orange scales. (**K**) Deletions at the site of *spalt* CRISPR (red box).

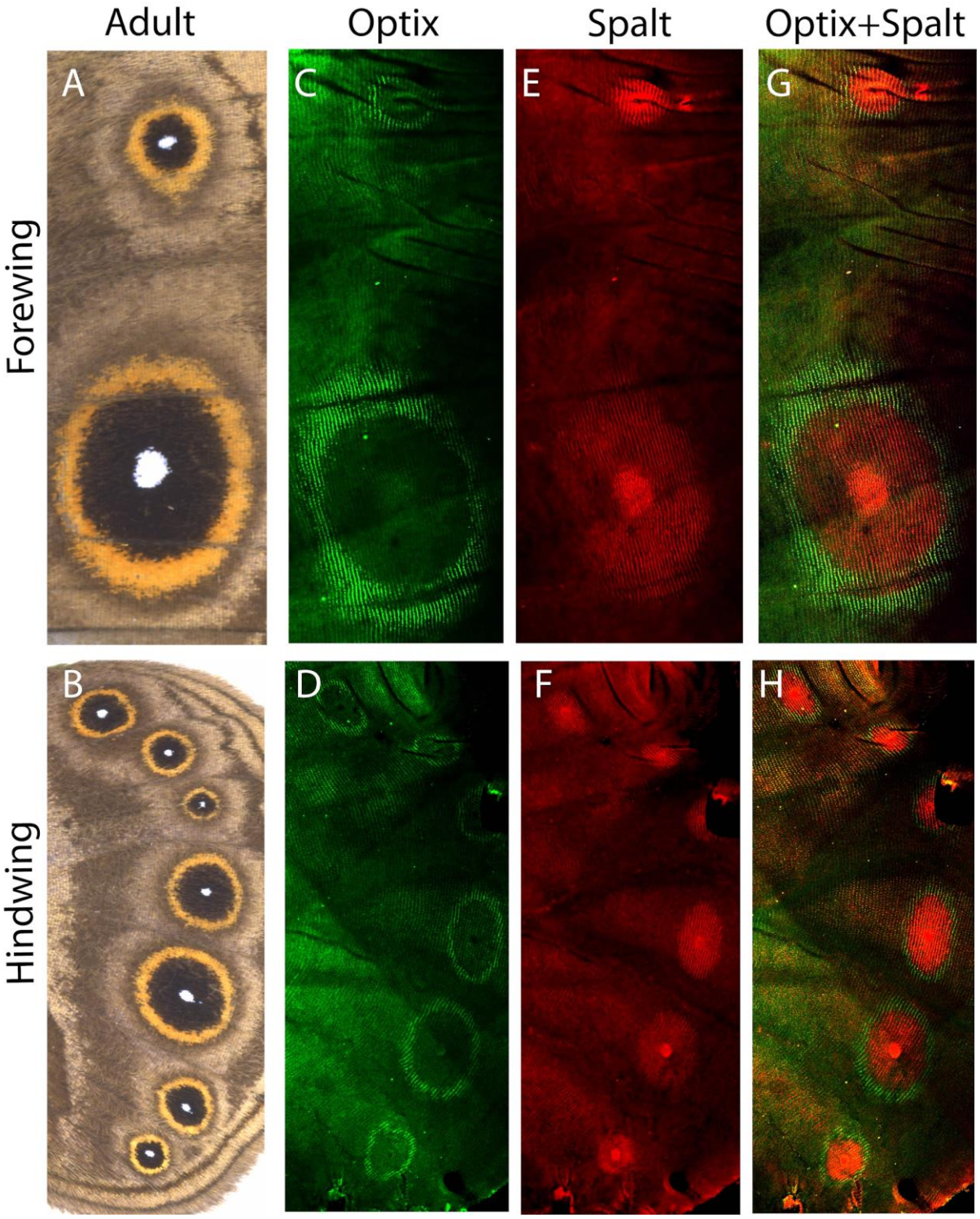

Figure S4. *Bicyclus* adult wings and the localization of Optix and Spalt proteins in 16-20 hrs old pupal wings. (**A and B**) Adult forewing and hindwing. (**C and D**) Optix localization in the forewing and hindwing. (**E and F**) Spalt localization in the forewing and hindwing. (**G and H**) Merged channels of Optix and Spalt.

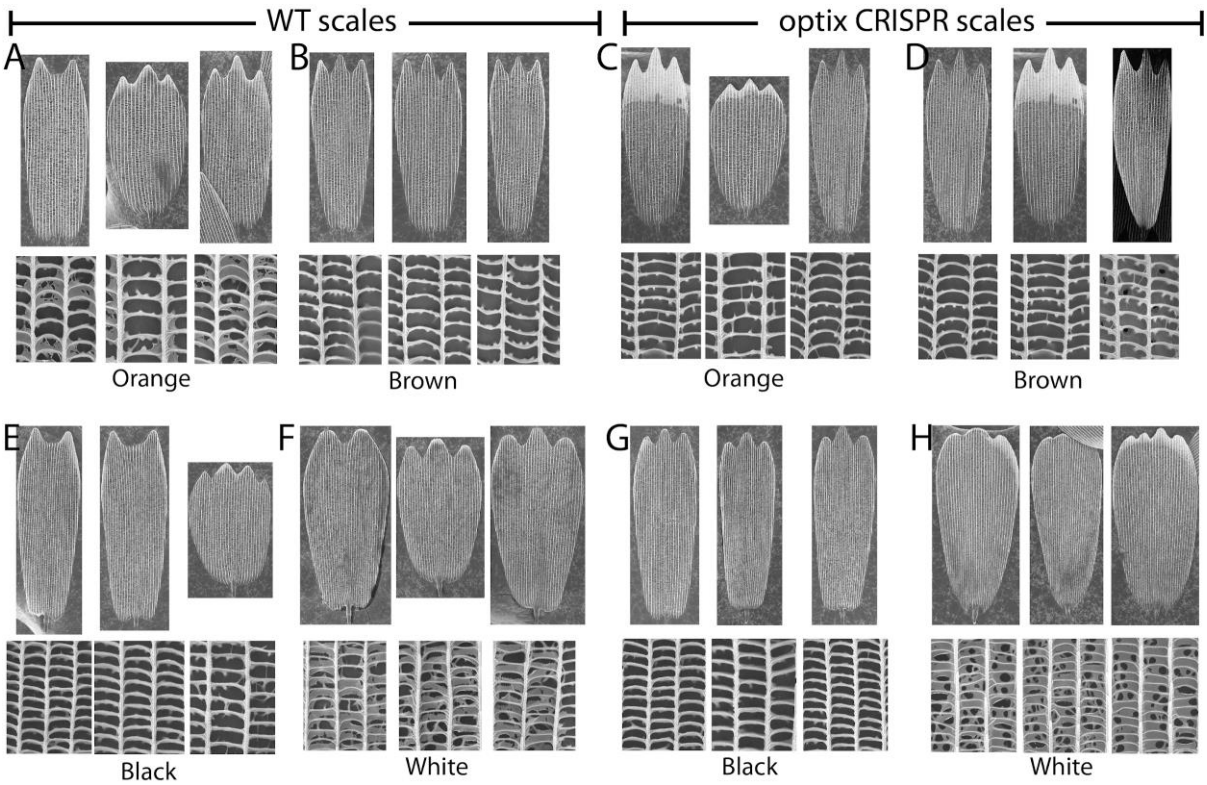

Figure S5. WT and *optix* CRISPR scale ultrastructures. WT orange (**A**) have higher amount of upper lamina in between the crossribs compared to *optix* CRISPR orange scales which became brown (**C**) and look similar to unaffected brown scales (**B and D**). There are no changes in the scale structure of black and white scale structures in between the WT and *optix* CRISPR (**E-H**).

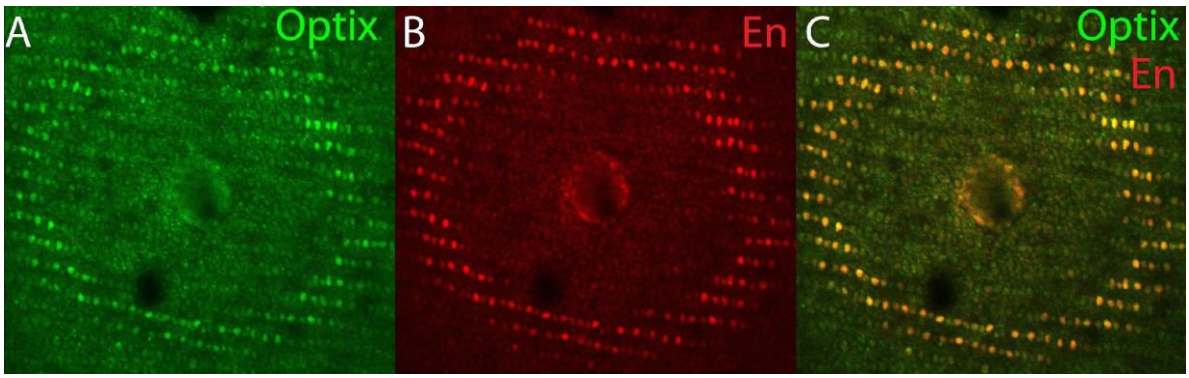

Figure S6. Co-localization of Optix and Engrailed (En) in the orange ring of the eyespots. Both (**A**) Optix and (**B**) En proteins are present in the cells that will form the orange scales of the eyespot.

Table S1: Primer table

Sl. No.	Name	Sequence
1.	dpp_insitu_F	GTTCTTCAACGTAAGCGGCG
2.	dpp_insitu_R	CCACAGCCTACCACCATCAT
3.	dpp_sequencing_F	GCCTGTTCTTCAACGTAAGC
4.	dpp_sequencing_R	CTCCGTGTACAGCATGAGC
5.	dpp_sequencing300_F	ACCGGCAGACAGAGACTG
6.	dpp_sequencing300_R	CCACTCCTCCTCCTCGTC
5.	optix_sequencing_F	AGACGCTGGAGGAGAGC
6.	optix_Sequencing_R	CGCTCGGTCTCTTTGC
7.	spalt_sequencing_F	GCATCGACAAGATGCTGAAA
8.	spalt_Sequencing_R	TTCATTTAGGGACGGTGGAG
9.	optix_CRISPR_1	GAAATTAATACGACTCACTATAGGGGCTTCGCAG CGCTCCAGCTGTTTTAGAGCTAGAAATAGC
10.	optix_CRISPR_2	GAAATTAATACGACTCACTATAGGTTCTTCGTCGG GTTCGGGTAGTTTTAGAGCTAGAAATAGC
11.	spalt_CRISPR_1	GAAATTAATACGACTCACTATAGGTGATCGAGCC GGCGTTGAGTTTTAGAGCTAGAAATAGC
12.	CRISPR_reverse	AAAAGCACCGACTCGGTGCCACTTTTT CAAGTTGATAACGGACTAGCCTTATTT TAACTTGCTATTTCTAGCTCTAAAAC
13.	dpp_siRNA_1	CAUCUAUAUCUAUGUUAUAUA UAUAACAUAGAUAUAGAUGAG
14.	dpp_siRNA_2	CUAUAUCUAUGUUAUAUAUGG AUAUAUAACAUAGAUAUAGAU
15.	dpp_qPCR_F	GCCGACGCAACTCTCATCTA
16.	dpp_qPCR_R	AGCCTACCACCATCATGTCC
17.	RpS18_F	ACTGCCATTAAGGGAGTCG
18.	Rps_18_R	TCACCAGCACGTTTATCCAA

Table S2. Optix CRISPR-Cas9 injection table

Sl. No.	Concentration	Date	Eggs Injected	Hatchlings	% Hatchlings
1.	300 ng/µl	6th June 2020	326	65	19.9
2.	300 ng/µl	9th July 2020	923	126	13.6
3.	300 ng/µl	27th Aug 2020	389	88	22.6

Table S3. Spalt CRISPR-Cas9 injection table

Sl. No.	Concentration	Date	Eggs Injected	Hatchlings	% Hatchlings
1.	300 ng/µl	23rd June 2020	276	39	14.1
2.	300 ng/µl	28th Aug 2020	593	74	12.5
3.	300 ng/µl	8th Sep 2020	879	106	12.1
4.	300 ng/µl	24th Sep 2020	726	65	9.0

Table S4. Immunofluorescence Buffers

Buffers	Chemicals	Amount
Fix buffer (30 ml)	0.1M PIPES pH 6.9 (500 mM)	6 ml
	1 mM EGTA pH 6.9 (500mM)	60 µl
	1% Triton x-100 (20 %)	1.5 ml
	2 mM $MgSO_4$ (1M)	60 µl
	37% Formaldehyde	55 µl per 500 µl of buffer
	dH_2O	22.4 ml
Block buffer (40 ml)	50 mM Tris pH 6.8 (1 M)	2 ml
	150 mM NaCl (5 M)	1.2 ml
	0.5% IGEPAL (NP40) (20%)	1 ml
	5 mg/ml BSA	0.2 gr
	H2O	35.8 ml
Wash buffer (200 ml)	50mM Tris pH 6.8 (1 M)	10 ml
	150 mM NaCl (5 M)	6 ml
	0.5% IGEPAL (20 %)	5 ml
	1 mg/ml BSA	0.2 gr
	dH_2O	179 ml
Mounting media	Tris-HCl (pH 9.2)	20 mM
	N-propyl gallate	0.5%
	Glycerol	60%

Table S5. *In-situ* hybridization Buffers

Buffers	Chemicals	Amount
10X PBS (500 ml) * Sterilize by autoclaving.	K_2HPO_4	5.34 g
	KH_2PO_4	2.64 g
	NaCl	40.9 g
	DEPC treated H_2O	To 500 ml
1X PBST (50 ml)	1X PBS	50 ml
	Tween® 20	50 µl
20X SSC (1000 ml) *Adjust the pH to 7.0 with 1M HCl and sterilize by autoclaving.	NaCl	175.3 g
	Trisodium citrate	88.2 g
	DEPC treated H_2O	Till 1000 ml
Pre-hybridization buffer (40 ml)	Formamide	20 ml
	20X SSC	10 ml
	DEPC treated water	10 ml
	TWEEN20	40 µl
Hybridization buffer (40 ml)	Formamide	20 ml
	20X SSC	10 ml
	DEPC treated water	10 ml
	TWEEN20	40 µl
	Salmon sperm	40 µl
	Glycine (100mg/ml)	40 µl
Block buffer (50 ml)	1X PBS	50 ml
	TWEEN20	50 µl
	BSA	0.1 gm
Alkaline phosphatase buffer (20 ml)	Tris-HCl (pH 8.0)	2 ml
	NaCl (5M)	400 µl
	$MgCl_2$ (200mM)	250 µl
	DEPC treated water	Till 20 ml
	TWEEN20	20 µl

Table S6: Cq values of the *dpp* RNAi qPCR experiment

Name	Cq1	Cq1	Cq3
dpp1(RNAi)	29.22	29.10	28.94
dpp2(RNAi)	28.78	28.77	28.58
dpp3(RNAi)	28.97	28.98	28.83
dpp4(RNAi)	26.66	26.53	26.48
dpp1(control)	28.44	28.51	28.46
dpp2(control)	28.11	28.17	28.06
dpp3(control)	28.23	28.18	28.18
dpp4(control)	26.14	26.11	26.17
RpS18_1(RNAi)	20.79	20.75	20.69
RpS18_2(RNAi)	20.43	20.36	20.32
RpS18_3(RNAi)	20.38	20.37	20.29
RpS18_4(RNAi)	19.43	19.39	19.33
RpS18_1(control)	21.06	21.03	21.07
RpS18_2(control)	20.11	20.15	20.11
RpS18_3(control)	19.55	19.58	19.53
RpS18_4(control)	19.27	19.22	19.21

Table S5. *In-situ* hybridization Buffers

Sequence of *decapentaplegic* used for *in-situ* hybridization.

GTTCTTCAACGTAAGCGGCGTACCGGCCGACGAGGTGGCGCGCGGCGCCGACCT
CTCGTTCCAACGAGCCGTCGGCACCACCGGCAGACAGAGACTGTTGTTGTACGA
CGTGGTGCGCCCTGGCCGCCGCGGCCACTCCGAGCCGATCCTGCGGCTGCTGGAC
TCCGTTCCGCTCCGGCCCGGGGAGGGAATCGTCAACGCCGACGCTCTGGGAGCG
GCGCGACGGTGGCTCAAAGAGCCCAAACATAATCACGGACTATTAGTGCGAGTG
TTAGAAGAAGACGCCGCGAGTGCGAGCAGGGACGCGAAGTTCCCGCACGTGCGC
GTGCGCAGACGCGTCACGGACGAGGAGGAGGAGTGGCGGACGGCGCAGCCGCT
GCTCATGCTGTACACGGAGGACGAGCGCGCGCGCGCGTCGCGGGAGACGAGCGA
GCGGCTGACGCGCAGCAAGCGCGCGGCGCAGCGGCGGGGGCACCGCGCGCACC
ACCGCCGCAAGGAGGCGCGCGAGATCTGCCAGCGCCGCCCGCTGTTCGTCGACT
TCGCGGACGTGGGCTGGAGCGACTGGATCGTGGCCCCGCACGGCTACGACGCGT
ACTACTGCCAGGGCGACTGCCCCTTCCCGCTGCCGGACCACCTCAACGGCACGA
ACCACGCGATAGTGCAGACTCTGGTCAACTCAGTGAACCCCGCGACGGTGCCCA
AAGCGTGCTGCGTGCCGACGCAACTCTCATCTATATCTATGTTATATATGGACGA
AGTGAACAATGTGGTGCTTAAAAACTATCAGGACATGATGGTGGTAGGCTGTGG

Region of *optix* used for CRISPR-Cas9 (Highlighted in red)

ATGCGCGGCTCCTGGGACGAGTCCACGACGGCGGCGCTGCACGCGCGCATCCTG
GAGGCGCACCGCGGGTCCGCCGCGCCCGACCGCGCCGAGCCCGCGTGCGAGCCT
CCGCCGCTGACGCTGGGCGCGCTGGAGCTGGCGGCGCCCACGCCGCTGCTGCCG
CTGCCCACGCTGAGCTTCAGCGCCGCGCAGGTGGCCACCGTGTGCGAGACGCTG
GAGGAGAGCGGCGACGTGGAGCGCCTGGCGCGCTTCTTGTGGTCGCTGCCCGTG
GCGCACCCCAACGTGGCCGAGCTGGAGCGCTGCGAAGCCGTGCTGCGCGCGCGC

GCCGTCGTCGCCTTCCACGCCGGCCGCCACCGCGAGCTGTACGCCATCCTCGAGC
GCCACCGCTTCCAGCGCTCCAGCCACGCCAAGCTGCAAGCGCTGTGGCTGGAGG
CGCACTACCAGGAGGCTGAGCGCCTGCGCGGCCGTCCGCTGGGCCCCGTCGACA
AGTACCGCGTGCGGAAGAAGTTCCCGCTCCCGAGGACGATCTGGGACGGCGAGC
AGAAGACGCACTGTTTCAAGGAGCGGACGCGATCTCTACTCCGAGAATGGTACC
TCCAAGATCCCTACCCGAACCCGACGAAGAAGAGGGAATTGGCGGCGGCGACGG
GTCTGACGCCGACGCAAGTCGGCAACTGGTTCAAAAACCGACGGCAAAGAGACC
GAGCGGCCGCCGCCAAGAACCGCTCCGCCGTGCTGGGCAGAGGATAA

Region of *spalt* targeted by CRISPR-Cas9 (location of guide RNA highlighted in red)

GCATCGACAAGATGCTGAAAATAATAATAGTCTCGAAGACGGCGAGGCCGAAAT
ACCTGAAGCCGACATGCCCCCCGTGGGTCTGCCGTTCCCTTTGGCAGGACACGTT
ACTCTTGAGGCTCTACAAAATACGAGAGTAGCGGTCGCCCAATTCGCTGCAACA
GCGATGGCAAATAATGCGAATAACGAAGCTGCTATACAAGAATTACAAGTGTTA
CACAACACTCTATACACTTTACAGTCACAACAAGTATTTCAACTTCAGTTAATAC
GTCAGCTTCAGAATCAGTTATCTCTAACTCGACGGAAAGAAGACGATCCACACA
GCCCACCGCCAAGTGAACCAGAACAGAATGCCCCGTCAACGCCGGCTCGATCAC
CGTCGCCGCCGCGTCCGCCACGGGAGCCGTCGCCTGTTATACCCTCTCCTCCTAC
TAGCCAAAGTTTGCCGTCGACTCACACACATCACACACCCAAAACTGAACAGAT
ATCTATCCCTAAGATTCCAACTTCCTCACCATCTTTAATGACCCACCCACTTTATA
GTTCAATTTCTTCGTCATTAGCATCTTCCATCATAACAAACAATGATCCTCCACCG
TCCCTAAATGAA

Region of *dpp* used for CRISPR-Cas9 (Highlighted in red)

ATGCGTGGGGCGTGCGCGTGCGCGGTGGTGTGCGCGTTGGTGGCGCTGTGCGCG
GCGCGGCTGGACGAGTCCGCGCGCGCCGCCGCCGAGAAGCAGCTGCTGGCACTG
CTGGGCCTGCCGCGCCGGCCGCCGCCGCGCGCCCGCCCGCCGCCCGTGCCGCGC
GCGCTGCGCGTGCTGTACGACTCGCGCGCGCTGCCCGCCGCCGCCGCCAACACG
GCGCGCTCCTTCCACCACACGCCCACGCCGCTCGACGAGCGCTTCCCCGGCGACC
ACCGCTTCCGCCTGTTCTTCAACGTAAGCGGCGTACCGGCCGACGAGGTGGCGCG
CGGCGCCGACCTCTCGTTCCAACGAGCCGTCGGCACCACCGGCAGACAGAGACT
GTTGTTGTACGACGTGGTGCGCCCTGGCCGCCGCGGCCACTCCGAGCCGATCCTG
CGGCTGCTGGACTCCGTTCCGCTCCGGCCCGGGGAGGGAATCGTCAACGCCGAC
GCTCTGGGAGCGGCGCGACGGTGGCTCAAAGAGCCCAAACATAATCACGGACTA
TTAGTGCGAGTGTTAGAAGAAGACGCCGCGAGTGCGAGCAGGGACGCGAAGTTC
CCGCACGTGCGCGTGCGCAGACGCGTCACGGACGAGGAGGAGGAGTGGCGGAC
GGCGCAGCCGCTGCTCATGCTGTACACGGAGGACGAGCGCGCGCGCGCGTCGCG
GGAGACGAGCGAGCGGCTGACGCGCAGCAAGCGCGCGGCGCAGCGGCGGGGGC
ACCGCGCGCACCACCGCCGCAAGGAGGCGCGCGAGATCTGCCAGCGCCGCCCGC
TGTTCGTCGACTTCGCGGACGTGGGCTGGAGCGACTGGATCGTGGCCCCGCACG
GCTACGACGCGTACTACTGCCAGGGCGACTGCCCCTTCCCGCTGCCGGACCACCT
CAACGGCACGAACCACGCGATAGTGCAGACTCTGGTCAACTCAGTGAACCCCGC
GACGGTGCCCAAAGCGTGCTGCGTGCCGACGCAACTCTCATCTATATCTATGTTA
TATATGGACGAAGTGAACAATGTGGTGCTTAAAAACTATCAGGACATGATGGTG
GTAGGCTGTGGCTGCCGATGA

R-code for the absorbance spectra analysis

```
setwd("…")
library(pavo)
specs <- getspec(where = getwd(), ext = "txt", lim = c(400, 750))
plot (specs, ylab = "Absorbance", col = rainbow(3))
specs <- procspec (specs, opt='smooth')
specs
spp <- substr(names(specs), 1, 4)
aggplot (specs, by=spp, ylab = "Absorbance")
```